EDGE ARTICLE

Check for updates

All publication charges for this article have been paid for by the Royal Society of Chemistry

Duplex-forming oligocarbamates with tunable nonbonding sites†

R. Kenton Weigel [ID] and Christopher A. Alabi [ID] *

In biopolymers such as proteins and nucleic acids, monomer sequence encodes for highly specific intra- and intermolecular interactions that direct self-assembly into complex architectures with high fidelity. This remarkable structural control translates into precise control over the properties of the biopolymer. Polymer scientists have sought to achieve similarly precise control over the structure and function of synthetic assemblies. A common strategy for achieving this goal has been to exploit existing biopolymers, known to associate with specific geometries and stoichiometries, for the assembly of synthetic building blocks. However, such systems are neither scalable nor amenable to the relatively harsh conditions required by various materials science applications, particularly those involving non-aqueous environments. To overcome these limitations, we have synthesized sequence-defined oligocarbamates (SeDOCs) that assemble into duplexes through complementary hydrogen bonds between thymine (**T**) and diaminotriazine (**D**) pendant groups. The SeDOC platform makes it simple to incorporate non-hydrogen-bonding sites into an oligomer's array of recognition motifs, thereby enabling an investigation into this unexplored handle for controlling the hybridization of complementary ligands. We successfully synthesized monovalent, divalent, and trivalent SeDOCs and characterized their self-assembly *via* diffusion ordered spectroscopy, ¹H-NMR titration, and isothermal titration calorimetry. Our findings reveal that the binding strength of monovalent oligomers with complementary pendant groups is entropically driven and independent of monomer sequence. The results further show that the hybridization of multivalent oligomers is cooperative, that their binding enthalpy (ΔH) and entropy ($T\Delta S$) depend on monomer sequence, and that sequence-dependent changes in ΔH and $T\Delta S$ occur in tandem to minimize the overall change in binding free energy.

Introduction

The precise placement of functional groups along a polymer chain plays a key role in encoding specific intra- and intermolecular interactions that direct self-assembly into discrete architectures. Directed folding and self-assembly in biopolymers like proteins and nucleic acids result in a wide array of properties that facilitate various biological functions, including cell scaffolding, templated synthesis, formation of biomolecular condensates, and information storage. Remarkably, these complex tasks are accomplished using polymers composed of a relatively small number of building blocks. Significant research efforts have been dedicated to producing synthetic systems that replicate the exquisite control over structure and function observed in their natural counterparts. An effective approach has been to exploit interactions optimized by nature to direct the assembly of various building blocks. Both protein–protein[1,2] and nucleic acid interactions[3–5] have been utilized to create precisely engineered nanostructures

via programmable self-assembly. DNA in particular has emerged as a powerful tool for constructing highly complex architectures, such as DNA origami,[6,7] because its base-pair specificity allows oligonucleotides to assemble with nanometer-scale precision.[8] This has been leveraged for directing the assembly of nano-particles (NPs) into well-organized structures[9] with applications as diagnostic[10–12] and therapeutic agents.[13,14] NP assemblies also hold significant promise for applications beyond the realm of biology, as they provide opportunities to precisely tailor material properties by manipulating NP size, shape, and the local arrangement of interacting ligands.[5,9]

Unfortunately, the widespread adoption of DNA-directed self-assembly for materials science applications is hindered by DNA's insolubility in organic solvents and the prohibitive cost of synthesizing DNA at the scale required for most nonbiological applications.[8] One approach to overcoming these limitations involves the synthesis of recognition-encoded oligomers with various chemistries that are soluble in the organic phase.[15] Similar to DNA, these ligands possess precisely positioned recognition sites along a sequence-defined backbone, enabling sequence-selective hybridization. Both dynamic-covalent bonds, such as imine,[16–19] boronic ester,[20–22] and Diels–Alder,[23] and noncovalent interactions such as hydrogen bonds,[24–27]

Robert Frederick Smith School of Chemical and Biomolecular Engineering, Cornell University, Ithaca, New York, USA. E-mail: caa238@cornell.edu

† Electronic supplementary information (ESI) available. See DOI: https://doi.org/10.1039/d4sc00242c

coordination bonds,[28–32] and salt bridges,[33–35] have been used to program self-assembly. The key feature of these bonds and interactions is their reversibility, which results in an equilibrium between unbound and hybridized ligands allowing mismatched complexes to reorganize into a preferred, low energy thermodynamic state. This equilibrium is characterized by an association constant, K_a, that quantifies the stability of the assembled structure. K_a is also a valuable metric for assessing selectivity by comparing the binding strengths of competing complexes. It is therefore important to understand the design principles that govern K_a in oligomeric assemblies, as this knowledge forms the foundation for leveraging recognition-encoded oligomers as building blocks for complex architectures.

In this study, we introduce a synthetic platform designed to generate sequence-defined oligomers capable of forming hybridized duplexes through complementary hydrogen bonding pendant groups. In contrast with previous studies that exclusively employ arrays of hydrogen bonding pendant groups to guide assembly,[25,36–43] we have incorporated non-hydrogen bonding sites into our oligomer's array of hydrogen bonding moieties to investigate their effect on hybridization. We show that these oligomers readily undergo duplex formation, and intriguingly, we observe that the number and location of nonbonding sites have a significant impact on the thermodynamics of binding.

Results and discussion

Recognition-encoded oligomers were produced with slight modifications to a scheme previously reported by the Alabi group for the gram-scale synthesis of sequence-defined oligocarbamates (SeDOCs) (Fig. 1).[44] In contrast to synthetic pathways where oligomers are synthesized from pre-existing monomers containing the recognition site, the platform employed in this study utilizes iterative reductive amination and carbamation reactions that enable independent tuning of each pendant group with a diverse array of compatible functionalities. The first generation of recognition encoded SeDOCs contain nonbonding methyl units (**m**) and complementary thymine (**T**) and diaminotriazine (**D**) pendant groups. **D** and **T** have been shown to form triple hydrogen bonds with a K_a of ~10^3 M^{-1} in chloroform.[45,46] The selection of the **D–T** motif was based on its K_a which allows fine-tuning of the overall binding affinity through incremental adjustment of the **D–T** valency (*i.e.*, the number of **D–T** interactions between a pair of oligomers). Furthermore, both **D** and **T** exhibit minimal self-dimerization, and their compact steric profiles ensure that they will not impede oligomer binding or negatively impact the synthesis of multivalent chains.

Synthesis

Primary amine-terminated diaminotriazine **2** and thymine **3** monomers were synthesized according to the reaction scheme in Fig. 1a and b. To obtain compound **2**, 2-chloro-4,6-diamino-1,3,5-triazine was refluxed with 2-(boc-amino)ethanethiol and potassium hydroxide. The resulting intermediate **1** was purified *via* flash chromatography and deprotected with trifluoroacetic acid. Compound **3** was synthesized by benzoyl-protecting the N(3) nitrogen[47] on thymine and reacting the N(1) nitrogen with 2-(boc-amino)ethyl bromide. Deprotection with trifluoroacetic acid afforded **3** in good yield. A library of ten SeDOC 3-mers (Fig. 2), each bearing three pendant groups, was generated to facilitate investigations into the effect of monovalent monomer sequence and **D–T** valency on the binding strength of
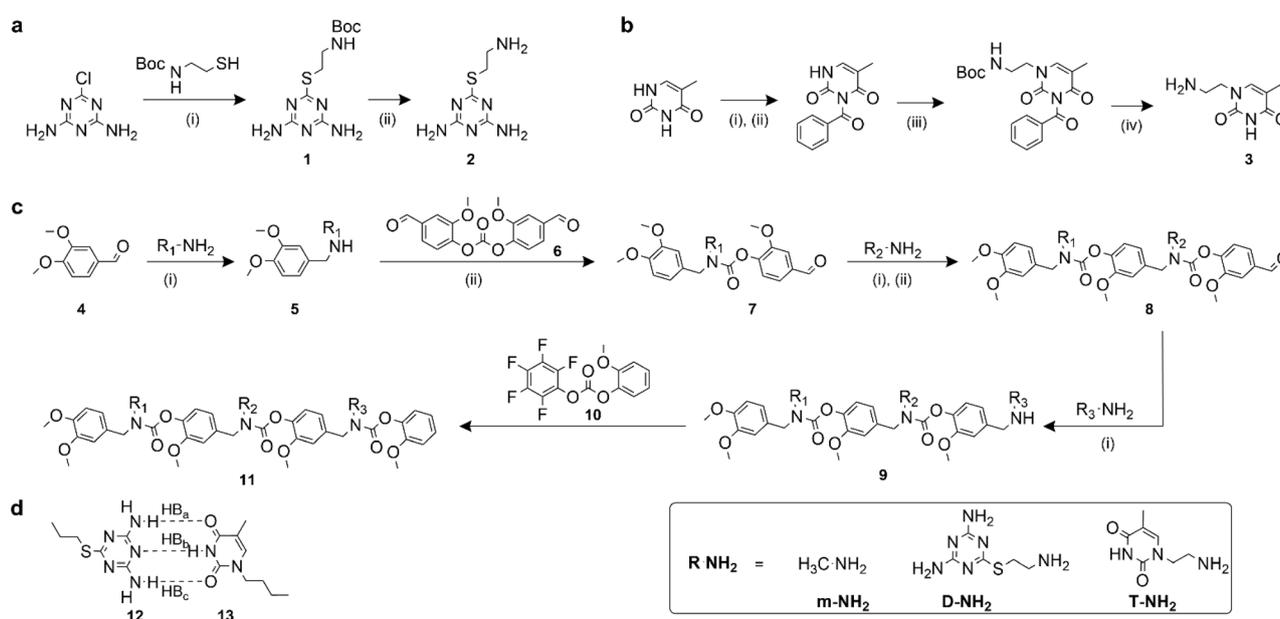

Fig. 1 Synthesis of SeDOC 3-mers and associated building blocks. (a), Synthesis of an amine-terminated diaminotriazine monomer. (i) Water/ethanol (1 : 1, v/v), KOH; (ii) TFA in CH$_2$Cl$_2$; (b), synthesis of amine-terminated thymine monomer. (i) Acetonitrile, pyridine, benzoyl chloride; (ii) 1,4-dioxane, KOH; (iii) 2-(boc-amino)ethyl bromide, K$_2$CO$_3$; (iv) TFA in CH$_2$Cl$_2$; (c), general SeDOC synthesis scheme (i) MeOH, AcOH, NaBH$_4$; (ii) divanillin carbonate, triethylamine, NH$_4$OH. (d), Watson–Crick-type hydrogen bond paring between a diaminotriazine (compound **12**) and thymine (compound **13**).
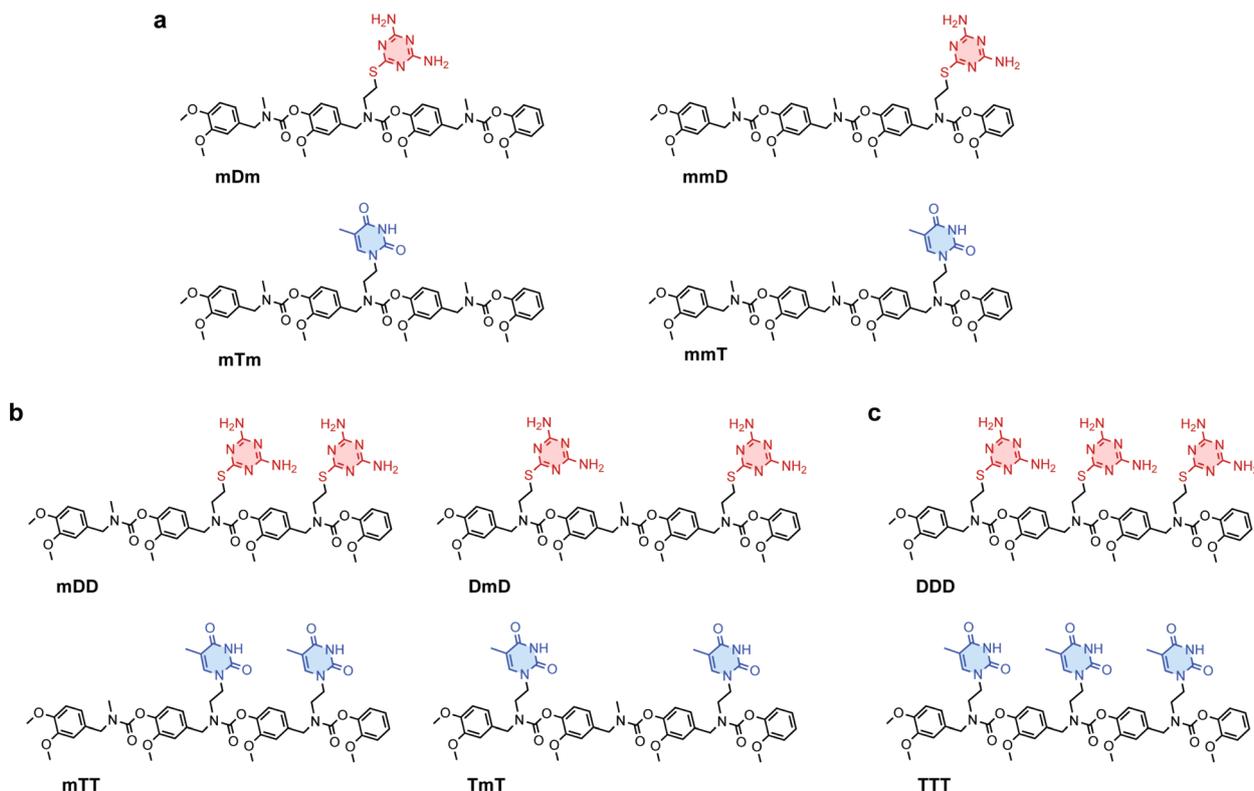
Fig. 2 Structures of (a), monovalent (b), divalent and (c), trivalent SeDOC oligomers.

complementary oligomers. SeDOC 3-mers were synthesized according to the iterative reaction pathway shown in Fig. 1c. 3,4-Dimethoxybenzaldehyde **4** was reacted with a primary amine-terminated **m**, **D**, or **T** (R–NH$_2$, Fig. 1c) and reduced with sodium borohydride. The resulting secondary-amine-terminated molecule **5** was reacted with divanillin carbonate **6** to regenerate the aldehyde end group **7** required for the addition of a second pendant group. Following a second reductive amination with the desired pendant group, the aldehyde was regenerated once again *via* acylation with **6** to give **8**. A final reductive amination was used to install the third desired pendant group and the ensuing secondary amine terminated oligomer **9** was reacted with pentafluorophenyl guaiacol carbonate **10** to generate the desired SeDOC **11**.

Detection of monovalent SeDOC hybridization *via* diffusion-ordered spectroscopy (DOSY)

Monovalent SeDOCs (*i.e.*, bearing a single diaminotriazine or thymine pendant group) were synthesized to study the effect of monovalent monomer sequence on K_a. We first confirmed *via* diffusion-ordered spectroscopy (DOSY) that SeDOCs with complementary pendant groups could hybridize.[48] According to the Stokes–Einstein equation, the diffusion coefficient scales with size. As such, unhybridized SeDOCs are expected to exhibit faster diffusion compared to the larger hybrid. The formation of a slow-diffusing species when ligands with complementary pendant groups are mixed is therefore indicative of hybridization. However, since rapid exchange between the unbound and

bound ligands outpaces the NMR timescale, the calculated diffusion coefficient from a specific peak in the NMR spectrum represents an ensemble average, incorporating contributions from both the hybrid and unbound ligand depending on their respective populations. To overcome this limitation, pairwise mixtures of oligomers with complementary pendant groups were prepared with an excess of one ligand (~3 : 1 mole ratio) to bias the limiting component towards the hybridized state. The diffusion coefficient was then calculated using resonances specific to the limiting component. Results of the DOSY experiments are shown in Fig. 3. The Stejskal–Tanner equation describes the relationship between the NMR signal strength (I), parameters related to the NMR experiment (b), and the diffusion coefficient (D_0):

$$I = I_0 e_0^{-bD} \tag{1}$$

where

$$b = \gamma^2 G^2 \delta^2 (\Delta - \delta/3) \tag{2}$$

γ is the gyromagnetic ratio, G is the gradient strength, δ is the gradient pulse length, and Δ is the mixing time. According to eqn (1), a plot of $\ln(I/I_0)$ *versus* b should give a line with a negative slope that can be used to obtain the diffusion coefficient (Fig. 3a–d). The DOSY results in Fig. 3a–h show that the diffusion coefficients of the pure ligands were similar, as anticipated given their similar size (**mDm** or **mmD** = 872 g
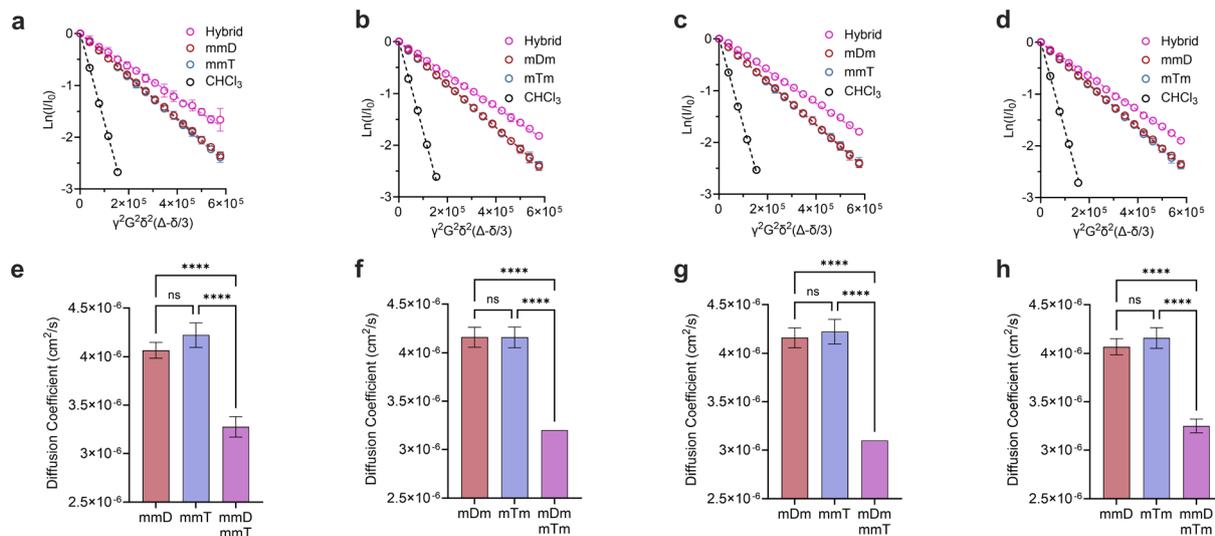
Fig. 3 Stesjkal−Tanner plots of (a), **mmD·mmT**; (b), **mDm mTm**; (c), **mDm mmT**; (d), **mmD·mTm** and their corresponding diffusion coefficients in (e−h). All DOSY experiments were performed in duplicates. Data are displayed as mean ± SD by one-way ANOVA. *$p < 0.033$, **$p < 0.0021$, ***$p < 0.0002$, ****$p < 0.0001$.

mol^{-1}, **mTm** or **mmT** = 855 g mol^{-1}). The data further reveals that within each mixture, the resonance specific to the limiting component exhibited a smaller diffusion coefficient than the corresponding pure ligand (Fig. 3e–h). This suggests that hybridization occurred between each complementary SeDOC pair. The diffusion coefficient of chloroform was the same across all samples, indicating that the observed reduction in SeDOC diffusion coefficient is not due to an elevated sample viscosity (Fig. 3a–d).

Hydrogen bonding between D and T confirmed *via* ^{1}H-NMR titration experiments

Having confirmed that monovalent SeDOCs with complementary pendant groups were assembling into larger hybrids, ^{1}H-NMR titration experiments were performed in CDCl$_3$ to determine whether hybridization was due to Watson-Crick hydrogen bonding between **D** and **T**. In these experiments, a **D** ligand (the titrant, **mDm** or **mmD**) was titrated into a **T** ligand (the titrand, **mTm** or **mmT**), and changes in the chemical shift of protons at the titrand's binding site were monitored as a function of mole ratio. A downfield shift upon titration is a classic indicator of hydrogen bonding between the titrand and titrant.[49] The **T** ligand was used as the titrand given the convenient location of thymine's NH peak, which appeared in a region of the spectrum with minimal spectral overlap. The NH peak in **mmT** alone gave rise to double signals which we attribute either to the presence of rotamers resulting from hindered rotation along the oligocarbamate backbone, or keto/enol thymine tautomers in relatively equal populations. Titrations were performed for each pairwise combination of monovalent oligomers with complementary pendant groups. In every experiment, the thymine NH proton shifted downfield from approximately 8.4 ppm in pure **T** ligand to approximately 12 ppm in a 3.5 : 1 **D** : **T** mixture (Fig. 4a, S42–S52†). The downfield shift of the thymine NH resonance was evidence that HB$_b$ (Fig. 1d) was forming. This indicated that

the slower diffusing species attributed to the hybridized oligomers in the DOSY experiments was due, at least in part, to hydrogen bonding between the **T** pendant group and **D** ligand. However, these titrations did not reveal the identity of thymine's hydrogen bonding partner, which could be the expected **D** pendant group, or the SeDOC backbone. To confirm that association was not caused by nonspecific hydrogen bonds with backbone acceptor sites, an additional experiment was performed in which mmm was titrated into **mmT**. The mmm SeDOC lacks hydrogen bonding pendant groups, so a downfield shift in T's donor proton upon titration would indicate the presence of hydrogen bonds with the oligocarbamate backbone. Fig. S53† shows that the addition of mmm did not cause a change in the chemical shift of thymine's NH, indicating that the downfield shift observed in titrations with complementary pendant groups (Fig. 4a, S42–S52†) could only be due to hydrogen bonds between D and T. While T does not hydrogen bond nonspecifically, ^{1}H-NMR titration (with mmm) and dilution experiments showed that D forms weak hydrogen bonds with the SeDOC backbone. However, these interactions have minimal impact on SeDOC hybridization because they are much weaker than the hydrogen bonds between D and T (Fig. S55–S58 and S65†).

Effect of monovalent monomer sequence on K_a assessed *via* isothermal titration calorimetry (ITC)

After establishing that monovalent SeDOCs undergo hybridization primarily driven by hydrogen bonding interactions between complementary **D** and **T** pendant groups, our next objective was to quantify the strength of hybridization and investigate how it varies with monomer sequence. As the exchange between the labile protons at the **D–T** binding site (including thymine's NH) could introduce errors in estimating binding strength *via* NMR titration (Fig. S44, S47, S50 and S52†), we opted instead for isothermal titration calorimetry (ITC),

which quantifies the heat absorbed or released during a binding event.[50] ITC experiments in this work were performed in chloroform and the resulting data were fit to an independent binding model to calculate K_a, ΔH, and the binding stoichiometry (n). This model describes the association of ligands due to interactions at a single recognition site or multiple equivalent sites. ΔG and ΔS were then calculated from eqn (3).

$$-RT \ln K_a = \Delta G = \Delta H - T\Delta S \qquad (3)$$

ITC revealed that monovalent SeDOCs with complementary pendant groups formed 1 : 1 duplexes (Fig. S63†). The binding strength of these duplexes ($\log K_a \approx 3.2$ M^{-1}) was independent of monomer sequence (Fig. 4b). In other words, a monovalent SeDOC, such as **mDm**, did not exhibit a strong preference for independent equilibrium binding to one sequence isomer, like **mTm**, over another, such as **mmT**. This suggests that there were no significant conformational differences between each pair of monovalent sequence isomers. ITC also showed that hybridization was both enthalpically ($\Delta H < 0$) and entropically ($\Delta S > 0$) favorable (Fig. 4c). While we expected that ΔH would be negative given the formation of hydrogen bonds between **D** and **T** pendant groups, the positive ΔS was unexpected. Hybridization typically leads to a decrease in entropy because it reduces the translational and conformational entropy of the binding partners. However, in the case of monovalent SeDOCs, hybridization was not only entropically favorable but also entropically driven. The value of $|T\Delta S|$ was approximately three to four times greater than $|\Delta H|$. While it is unusual to observe an increase in entropy upon hybridization, there are examples of systems that display this phenomenon.[51,52] A common feature of these systems is that they have small binding enthalpies ($\Delta H > -15$ kJ mol^{-1}), which is theorized to limit the loss of translational and conformational entropy experienced by the binding partners upon hybridization.[51,53] If this decrease is sufficiently small, it can be overcome by favorable sources of entropy so that the overall ΔS is positive.

Given that ITC measures the change in entropy of the entire system (*i.e.*, oligomers and solvent), the observed increase in entropy could arise from an increase in the solvent's entropy, the oligomer(s)' entropy, or a combination of both. An increase

in solvent entropy could occur upon hybridization if solvent ordering was present around the SeDOCs in the unbound state. Solvent release upon hybridization would then contribute to an increase in both translational and configurational entropy. To investigate further, an ITC experiment was performed in acetonitrile to determine whether hybridization remained entropically favorable (Fig. S66†). Interestingly, the ITC results showed that binding of **mDm** to **mTm** in acetonitrile still led to an increase in entropy. Acetonitrile, like chloroform, can hydrogen bond[54] with the oligomers and so this experiment does not rule out solvent effects as the source of $\Delta S > 0$. However, it demonstrated that the phenomenon is not unique to chloroform. Unfortunately, limited SeDOC solubility in inert solvents prevented hybridization experiments from being investigated more broadly.

To investigate the SeDOC backbone's role in hybridization, free-standing thymine (compound **12**, **T**) and diaminotriazine (compound **13**, **D**) monomers were synthesized (Fig. 1D). Hybridization of these monomers was analyzed by ITC experiments in chloroform. The results showed that hybridization was still entropically favorable (Fig. S67†) indicating that the positive change in entropy cannot be solely attributed to backbone effects. Additional computational studies are underway to shed light on the factors that contribute to the entropically driven hybridization of monovalent SeDOCs.

Assessing K_a, ΔH and ΔS of multivalent ligands

Divalent and trivalent SeDOCs (Fig. 2) were synthesized to investigate the impact of valency and sequence on K_a. In cases where interactions between a pair of ligands are cooperative, increasing the valency can lead to a substantial increase in binding strength of an order of magnitude or more. Hybridization of **mDD** with **mTT**, **DmD** with **TmT**, and **DDD** with **TTT** was confirmed *via* DOSY in CDCl$_3$ for **mDD·mTT** and **DmD·TmT**, and in CDCl$_3$/MeOD (9 : 1, v/v) for **DDD·TTT**. Stejskal–Tanner plots revealed that the hybrids diffused slower than their pure, unbound constituents, as evidenced by the hybrids' shallower slope (Fig. 5a–c) and the resulting quantified diffusion coefficients (Fig. 5e–g). ITC experiments in chloroform were used to measure the thermodynamic parameters of each binding event. Fitting the ITC data to an independent binding model revealed that **mDD** and **mTT** formed 1 : 1
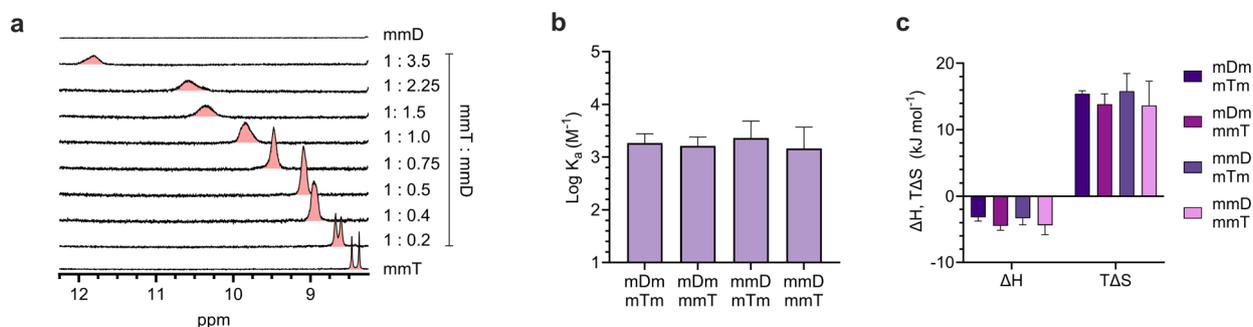

Fig. 4 (a). ^{1}H-NMR titration experiment between **mmT** and **mmD** in CDCl$_3$ showed a downfield shift in **mmT**'s NH proton. (b). Binding strength, *i.e.* association constants (K_a), of monovalent hybrids measured by ITC. (c). Thermodynamic binding parameters of monovalent SeDOCs with complementary pendant groups measured *via* ITC in chloroform.
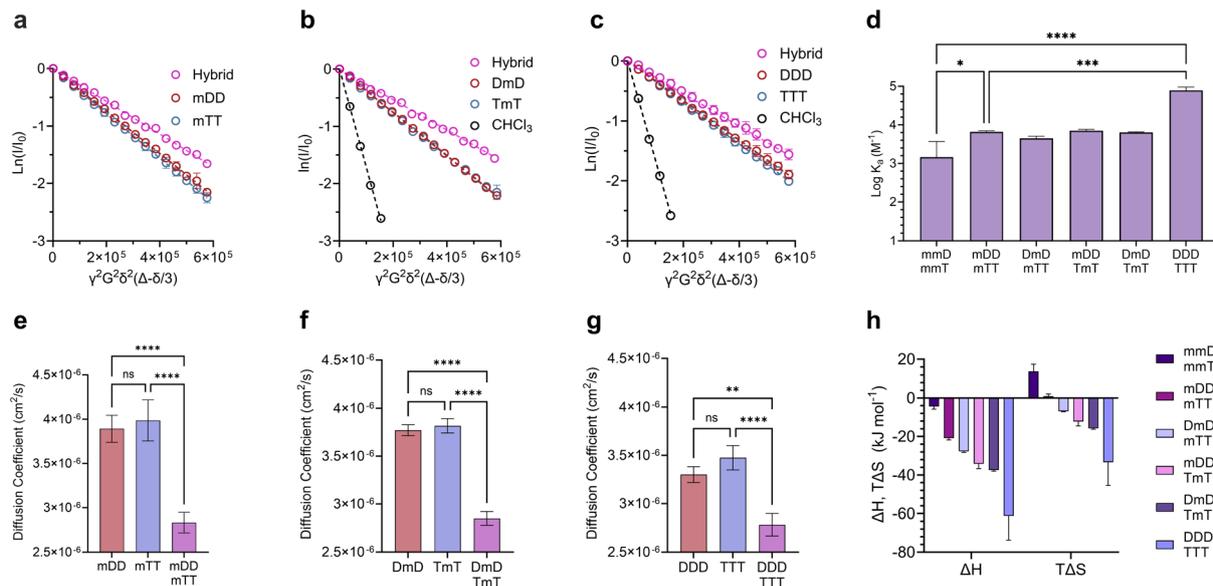
Fig. 5 Characterization of di- and trivalent SeDOC hybrids. Stejskal–Tanner plots comparing diffusion coefficients of (a), **mDD**, **mTT**, and **mDD·mTT**. (b), **DmD**, **TmT**, and **DmD·TmT**. (c), **DDD**, **TTT**, and **DDD·TTT**. (d), log K_a values of di- and trivalent SeDOC hybrids measured by ITC. (e–g), Diffusion coefficients of pure mono, di- and trivalent SeDOCs and the corresponding hybrids. Diffusion coefficients obtained from slopes in plots in (a–c). (h), Thermodynamic binding parameters of multivalent SeDOCs with complementary pendant groups measured *via* ITC. Data are displayed as mean ± SD by one-way ANOVA. *$p < 0.033$, **$p < 0.0021$, ***$p < 0.0002$, ****$p < 0.0001$.

duplexes with a log K_a of 3.8 M^{-1} (Fig. 5d). ΔH decreased from approximately -4 kJ mol^{-1} in the monovalent hybrids to -20.8 kJ mol^{-1} in **mDD·mTT** (Fig. 5h). This significant decrease in binding enthalpy points to the formation of an additional set of hydrogen bonds between **mDD** and **mTT** relative to their monovalent counterparts. However, the strengthening of the enthalpic term did not lead to as large increase in K_a as expected because **mDD·mTT** had a diminished entropic driving force. $T\Delta S$ was significantly reduced, from roughly 14 kJ mol^{-1} in the monovalent hybrids to 0.9 kJ mol^{-1} in **mDD·mTT**.

Log K_a values of **DmD·TmT** and **mDD·TmT** were similar to that of **mDD·mTT** (log $K_a = 3.8$ M^{-1}). **DmD·mTT** (log $K_a = 3.6$ M^{-1}) was slightly less stable than the other divalent duplexes, however this difference was not statistically significant (Fig. 5f). Though log K_a did not vary with sequence, there were sequence-dependent differences in the entropic and enthalpic contributions to their binding free energies. The complexes were equally stable despite these differences because stronger enthalpic interactions were offset by increased entropic penalties. For example, **DmD·TmT** had both the strongest enthalpic interactions ($\Delta H = -37.2$ kJ mol^{-1}) of the three and the greatest adverse entropy ($T\Delta S = -15.4$ kJ mol^{-1}). Similarly, **mDD·TmT** ($\Delta H = -34.2$ kJ mol^{-1}) had both a weaker enthalpic driving force than **DmD·TmT** and a smaller entropic cost ($T\Delta S = -12.2$ kJ mol^{-1}) (Fig. 5f). These differences in ΔH and ΔS were observed despite each complex having the same maximum number of **D–T** interactions, and could be attributed to electronic or conformational effects that vary with sequence.

Adding a third **D–T** interaction between the 3-mers, as represented in **DDD·TTT**, increased the log K_a to 4.9 M^{-1}. This large increase in binding strength was indicative of a cooperative binding mechanism as K_a was over an order of magnitude

greater than that of **mDD·mTT**. The increase in K_a was due to a substantial decrease in ΔH, from -20.8 kJ mol^{-1} in **mDD·mTT** and -37.2 kJ mol^{-1} in **DmD·TmT** to -61.3 kJ mol^{-1} in **DDD·TTT**. The large change in ΔH suggests that **DDD** and **TTT** formed three sets of hydrogen bonds to give a fully zipped-up duplex. The formation of this duplex came with a significant entropic penalty, with $T\Delta S = -33.4$ kJ mol^{-1} (Fig. 5h).

We hypothesize that $T\Delta S$ was diminished in the divalent duplexes compared to the monovalent hybrids because the second **D–T** interaction created an additional anchor point between the ligands which limited the conformations accessible to the duplex. The enhanced enthalpic interactions also rigidified the structure by limiting vibrations between the hybridized ligands.[55] For similar reasons, ΔS decreased even further in the trivalent case. The reduction in conformational flexibility of the di- and trivalent duplexes compared to their unbound states, along with the presence of strong hydrogen bonds, significantly outweighed other effects likely responsible for the positive entropy observed in the monovalent ligands.

Formation of mixed-mode hybrids

Mixed-mode ITC experiments were performed to assess how K_a, ΔH, and $T\Delta S$ varied in hybrids of ligands with differing valency (Fig. 6). As expected, increasing the total number of **D–T** units in a hybridized duplex led to an increase in K_a (Fig. 6a). However, the relative size of K_a was dependent on the magnitudes of ΔH and $T\Delta S$. By comparing the ΔH values of "matched" complexes (*e.g.*, **mmD·mmT**, **mDD·mTT**) with those of "mismatched" complexes (*e.g.*, **mmD·mTT**, **mDD·TTT**), we determined that matched hybrids were indeed engaging in the maximum number of available hydrogen bonds. Hybridization of **mmD**
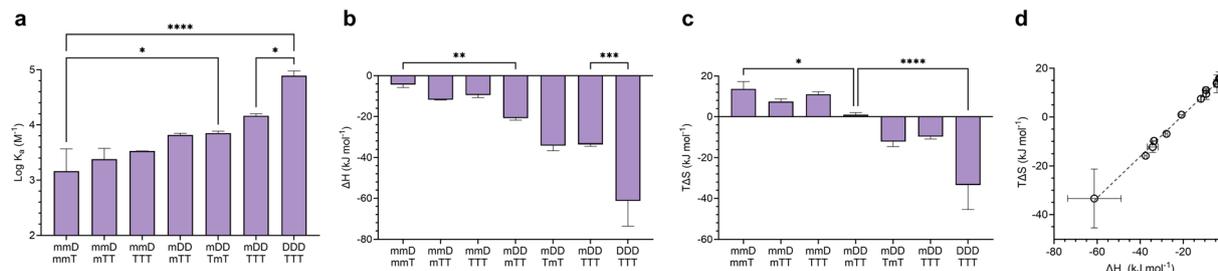
Fig. 6 (a–c), Binding thermodynamics of mixed-mode hybrids compared to complementary mono-, di-, and trivalent complexes. (d), Enthalpy versus entropy plot of D–T and SeDOC complexes in chloroform. Data are displayed as mean ± SD by one-way ANOVA. $*p < 0.033$, $**p < 0.0021$, $***p < 0.0002$, $****p < 0.0001$.

with divalent **mTT** or trivalent **TTT** was expected to have a slightly stronger enthalpic term than the **mmD·mmT** hybrid ($\Delta H = -4.4$ kJ mol^{-1}) due to the presence of a neighboring **T** binding site. We also anticipated that **mmD·mTT** ($\Delta H = -11.8$ kJ mol^{-1}) would have a weaker ΔH than **mDD·mTT** ($\Delta H = -20.8$ kJ mol^{-1}) and **mDD·TmT** ($\Delta H = -34.2$ kJ mol^{-1}) because **mmD** can only form a single set of hydrogen bonds. While it appeared that these trends were observed, the error associated with the measurements prevented the binding enthalpy of **mmD·mTT** from being statistically different from those of **mmD·mmT** or **mDD·mTT** (Fig. 6b). Similarly, the ΔH of **mDD·mTT** and **mDD·TmT** was weaker than **mDD·TTT** ($\Delta H = -33.6$ kJ mol^{-1}) due to the latter's additional **T** site. Finally, a statistically significant difference was observed between the enthalpic terms of **mDD·TTT** and **DDD·TTT**, thus confirming that **DDD·TTT** had formed a three-rung molecular ladder. We also examined the entropic favorability of both matched and mismatched hybrids. We observed minimal changes in $T\Delta S$ in duplexes formed between **mmD** and thymine-containing SeDOCs, *i.e.*, **mmT**, **mTT** and **TTT** (Fig. 6c). In contrast, a significant decrease in entropy was observed in duplexes formed between two multivalent SeDOCs. Since strengthening the enthalpic interactions reduces the amount of residual motion retained by the complex, we expected the binding entropy of **mDD·mTT** to be more positive than **mDD·TTT**, and this was observed. Similarly, **DDD·TTT** was predicted to be the least conformationally flexible oligomer, *i.e.*, most negative $T\Delta S$, because it has the greatest number of interactions between binding partners.

A plot of all ΔH values against $T\Delta S$ is shown in Fig. 6d. This data shows that SeDOCs exhibit enthalpy-entropy compensation, a phenomenon characterized by a linear relationship between ΔH and $T\Delta S$.[56,57] Enthalpy–entropy compensation is observed within a family of similar compounds, as seen here with our SeDOCs, when an increase in the exothermicity of a noncovalent association leads to a decrease in entropy (or *vice versa*) that offsets the resulting change in binding free energy.[58] This compensation effect has been observed in a number of other systems, including in the binding of neutral molecules to macrocycles in dichloromethane,[51,59] the binding of protein-ligand complexes,[60] and the gas-phase complexation of iodine with organic donor molecules,[61] just to name a few. The molecular basis of this phenomenon is still under debate, with

possible explanations invoking solvent structure, a consequence of finite specific heat capacities, multiple weak interactions, or even an evolutionary driven condition for thermodynamic homeostasis. Molecular dynamic simulations are key to providing the connection between these macroscopic extra-thermodynamic correlations and their molecular structure and dynamic determinants.

Conclusions

This body of work demonstrates that SeDOCs encoded with **D** and **T** moieties have the capacity to assemble into macromolecular duplexes through the formation of hydrogen bonds between complementary pendant groups. Hybridization of mono-, di-, and trivalent SeDOC 3-mers with complementary pendant groups was first identified using DOSY, as evidenced by a reduction in the diffusion coefficient of the duplex. ^{1}H-NMR titration experiments provided further evidence that these hybrids resulted from hydrogen bonding interactions between **D** and **T** units, rather than non-specific interactions with the SeDOC backbone. Thermodynamic binding parameters measured *via* ITC revealed that K_a, ΔH, and ΔS did not vary with monovalent monomer sequence. Surprisingly, hybridization of monovalent oligomers was entropically driven ($T\Delta S \gg |\Delta H|$). Divalent oligomers formed stronger hybrids that were facilitated by the second set of hydrogen bonds that formed between the ligands. There were sequence-dependent differences in the enthalpic and entropic contributions to the binding free energies of divalent hybrids though their $\log K_a$ remained similar. The K_a of the trivalent SeDOC hybrids, **DDD·TTT** ($\log K_a = 4.9$ M^{-1}), was over an order of magnitude greater than that of the divalent duplexes, indicative of a cooperative binding mechanism. Mixed-mode ITC experiments provided evidence that the duplexes were forming the maximum possible number of available hydrogen bonds. Increasing the number of hydrogen bonding motifs in a duplex eventually led to a decrease in entropy upon hybridization. We attribute this negative ΔS to the increased rigidity of the duplex and the strong collective hydrogen bonds that limit residual motion. Finally, we observe a linear relationship between ΔH and $T\Delta S$, commonly characterized as enthalpy–entropy compensation, which minimizes large changes to the resulting free energy term. In conclusion, this study offers a comprehensive exploration of the

thermodynamic principles governing SeDOC association through **D–T** interactions and establishes a solid groundwork for harnessing recognition-encoded SeDOCs as fundamental building blocks for the assembly of higher-order architectures.

Data availability

The data supporting the findings, including NMR and LCMS characterization of SeDOC building blocks and 3-mers, ^{1}H-NMR titration data, and ITC data are available in the ESI.†

Author contributions

RKW performed the experiments, analyzed the data, and wrote the manuscript. CAA conceptualized the research, validated the data, and edited the manuscript.

Conflicts of interest

There are no conflicts to declare.

Acknowledgements

Notes and references

1 K.-H. Kim, D.-K. Ko, Y.-T. Kim, N. H. Kim, J. Paul, S.-Q. Zhang, C. B. Murray, R. Acharya, W. F. DeGrado, Y. H. Kim and G. Grigoryan, *Nat. Commun.*, 2016, **7**, 11429.

2 B. E. Barnes, T. A. Jenkins, L. M. Stein, R. T. Mathers, M. Wicaksana, M. A. Pasquinelli and D. A. Savin, *Biomacromolecules*, 2020, **21**, 2463–2472.

3 Z. J. Gartner and D. R. Liu, *J. Am. Chem. Soc.*, 2001, **123**, 6961–6963.

4 Z. J. Gartner, B. N. Tse, R. Grubina, J. B. Doyon, T. M. Snyder and D. R. Liu, *Science*, 2004, **305**, 1601–1605.

5 S. Y. Park, A. K. R. Lytton-Jean, B. Lee, S. Weigand, G. C. Schatz and C. A. Mirkin, *Nature*, 2008, **451**, 553–556.

6 P. W. K. Rothemund, *Nature*, 2006, **440**, 297–302.

7 D. Han, X. Qi, C. Myhrvold, B. Wang, M. Dai, S. Jiang, M. Bates, Y. Liu, B. An, F. Zhang, H. Yan and P. Yin, *Science*, 2017, **358**, 6369.

8 A. V. Pinheiro, D. Han, W. M. Shih and H. Yan, *Nat. Nanotechnol.*, 2011, **6**, 763–772.

9 R. J. Macfarlane, B. Lee, M. R. Jones, N. Harris, G. C. Schatz and C. A. Mirkin, *Science*, 2011, **334**, 204–208.

10 R. Elghanian, J. J. Storhoff, R. C. Mucic, R. L. Letsinger and C. A. Mirkin, *Science*, 1997, **277**, 1078–1081.

11 J.-M. Nam, C. S. Thaxton and C. A. Mirkin, *Science*, 2003, **301**, 1884–1886.

12 D. S. Seferos, D. A. Giljohann, H. D. Hill, A. E. Prigodich and C. A. Mirkin, *J. Am. Chem. Soc.*, 2007, **129**, 15477–15479.

13 N. W. S. Kam, M. O'Connell, J. A. Wisdom and H. Dai, *Proc. Natl. Acad. Sci. U. S. A.*, 2005, **102**, 11600–11605.

14 G. von Maltzahn, J.-H. Park, K. Y. Lin, N. Singh, C. Schwöppe, R. Mesters, W. E. Berdel, E. Ruoslahti, M. J. Sailor and S. N. Bhatia, *Nat. Mater.*, 2011, **10**, 545–552.

15 R. K. Weigel, A. Rangamani and C. A. Alabi, *Nat. Rev. Chem*, 2023, **7**, 875–888.

16 C. S. Hartley, E. L. Elliott and J. S. Moore, *J. Am. Chem. Soc.*, 2007, **129**, 4512–4513.

17 E. L. Elliott, C. S. Hartley and J. S. Moore, *Chem. Commun.*, 2011, **47**, 5028.

18 M. M. Cencer, A. J. Greenlee and J. S. Moore, *J. Am. Chem. Soc.*, 2020, **142**, 162–168.

19 T. Wei, J. C. Furgal, J. H. Jung and T. F. Scott, *Polym. Chem.*, 2017, **8**, 520–527.

20 M. Hebel, A. Riegger, M. M. Zegota, G. Kizilsavas, J. Gačanin, M. Pieszka, T. Lückerath, J. A. S. Coelho, M. Wagner, P. M. P. Gois, D. Y. W. Ng and T. Weil, *J. Am. Chem. Soc.*, 2019, **141**, 14026–14031.

21 M. F. Dunn, T. Wei, R. N. Zuckermann and T. F. Scott, *Polym. Chem.*, 2019, **10**, 2337–2343.

22 M. M. Zegota, M. A. Müller, B. Lantzberg, G. Kizilsavas, J. A. S. Coelho, P. Moscariello, M. Martínez-Negro, S. Morsbach, P. M. P. Gois, M. Wagner, D. Y. W. Ng, S. L. Kuan and T. Weil, *J. Am. Chem. Soc.*, 2021, **143**, 17047–17058.

23 S. C. Leguizamon, A. F. Alqubati and T. F. Scott, *Polym. Chem.*, 2020, **11**, 7714–7720.

24 E. A. Archer and M. J. Krische, *J. Am. Chem. Soc.*, 2002, **124**, 5074–5083.

25 A. E. Stross, G. Iadevaia and C. A. Hunter, *Chem. Sci.*, 2016, **7**, 94–101.

26 G. Iadevaia and C. A. Hunter, *Acc. Chem. Res.*, 2023, **56**, 712–727.

27 H. Zeng, X. Yang, A. L. Brown, S. Martinovic, R. D. Smith and B. Gong, *Chem. Commun.*, 2003, 1556.

28 A. Marquis, V. Smith, J. Harrowfield, J. Lehn, H. Herschbach, R. Sanvito, E. Leize-Wagner and A. Van Dorsselaer, *Chem.–Eur. J.*, 2006, **12**, 5632–5641.

29 J. M. Lehn, A. Rigault, J. Siegel, J. Harrowfield, B. Chevrier and D. Moras, *Proc. Natl. Acad. Sci. U. S. A.*, 1987, **84**, 2565–2569.

30 R. Kramer, J. M. Lehn and A. Marquis-Rigault, *Proc. Natl. Acad. Sci. U. S. A.*, 1993, **90**, 5394–5398.

31 V. C. M. Smith and J.-M. Lehn, *Chem. Commun.*, 1996, 2733.

32 B. Hasenknopf and J.-M. Lehn, *Helv. Chim. Acta*, 1996, **79**, 1643–1650.

33 H. Ito, Y. Furusho, T. Hasegawa and E. Yashima, *J. Am. Chem. Soc.*, 2008, **130**, 14008–14015.

34 J. Sánchez-Quesada, C. Seel, P. Prados, J. de Mendoza, I. Dalcol and E. Giralt, *J. Am. Chem. Soc.*, 1996, **118**, 277–278.

35 Y. Tanaka, H. Katagiri, Y. Furusho and E. Yashima, *Angew. Chem.*, 2005, **117**, 3935–3938.

36 G. Iadevaia, A. E. Stross, A. Neumann and C. A. Hunter, *Chem. Sci.*, 2016, **7**, 1760–1767.

37 A. E. Stross, G. Iadevaia and C. A. Hunter, *Chem. Sci.*, 2016, **7**, 5686–5691.

38 D. Núñez-Villanueva, G. Iadevaia, A. E. Stross, M. A. Jinks, J. A. Swain and C. A. Hunter, *J. Am. Chem. Soc.*, 2017, **139**, 6654–6662.

39 A. E. Stross, G. Iadevaia, D. Núñez-Villanueva and C. A. Hunter, *J. Am. Chem. Soc.*, 2017, **139**, 12655–12663.

40 G. Iadevaia, D. Núñez-Villanueva, A. E. Stross and C. A. Hunter, *Org. Biomol. Chem.*, 2018, **16**, 4183–4190.

41 F. T. Szczypiński and C. A. Hunter, *Chem. Sci.*, 2019, **10**, 2444–2451.

42 F. T. Szczypiński, L. Gabrielli and C. A. Hunter, *Chem. Sci.*, 2019, **10**, 5397–5404.

43 P. Troselj, P. Bolgar, P. Ballester and C. A. Hunter, *J. Am. Chem. Soc.*, 2021, **143**, 8669–8678.

44 E. A. Hoff, G. X. De Hoe, C. M. Mulvaney, M. A. Hillmyer and C. A. Alabi, *J. Am. Chem. Soc.*, 2020, **142**, 6729–6736.

45 F. H. Beijer, R. P. Sijbesma, J. A. J. M. Vekemans, E. W. Meijer, H. Kooijman and A. L. Spek, *J. Org. Chem.*, 1996, **61**, 6371–6380.

46 T. K. Park, J. Schroeder and J. Rebek, *J. Am. Chem. Soc.*, 1991, **113**, 5125–5127.

47 J. Zhou and P. B. Shevlin, *Synth. Commun.*, 1997, **27**, 3591–3597.

48 P. Groves, *Polym. Chem.*, 2017, **8**, 6700–6708.

49 M. N. C. Zarycz and C. Fonseca Guerra, *J. Phys. Chem. Lett.*, 2018, **9**, 3720–3724.

50 W. R. Archer and M. D. Schulz, *Soft Matter*, 2020, **16**, 8760–8774.

51 D. H. Williams and M. S. Westwell, *Chem. Soc. Rev.*, 1998, **27**, 57.

52 A. Camara-Campos, C. A. Hunter and S. Tomas, *Proc. Natl. Acad. Sci. U. S. A.*, 2006, **103**, 3034–3038.

53 J. D. Dunitz, *Chem. Biol.*, 1995, **2**, 709–712.

54 R. Gopi, N. Ramanathan and K. Sundararajan, *J. Mol. Struct.*, 2015, **1094**, 118–129.

55 D. H. Williams, N. L. Davies and J. J. Koivisto, *J. Am. Chem. Soc.*, 2004, **126**, 14267–14272.

56 U. Ryde, *Med. Chem. Commun.*, 2014, **5**, 1324–1336.

57 D. M. Ford, *J. Am. Chem. Soc.*, 2005, **127**, 16167–16170.

58 F. Peccati and G. Jiménez-Osés, *ACS Omega*, 2021, **6**, 11122–11130.

59 R. M. Izatt, J. S. Bradshaw, K. Pawlak, R. L. Bruening and B. J. Tarbet, *Chem. Rev.*, 1992, **92**, 1261–1354.

60 C. H. Reynolds and M. K. Holloway, *ACS Med. Chem. Lett.*, 2011, **2**, 433–437.

61 M. S. Searle, M. S. Westwell and D. H. Williams, *J. Chem. Soc., Perkin Trans. 2*, 1995, 141–151.